ISBN: 978-3-95450-210-3 doi:10.18429/JACoW-FEL2019-TUP087

START-TO-END SIMULATIONS OF THE REFLECTION HARD X-RAY SELF-SEEDING AT THE SHINE PROJECT *

Tao Liu†, Chao Feng, Xiaohao Dong
Shanghai Advanced Research Institute, Chinese Academy of Sciences, Shanghai 201210, China

Abstract

The Shanghai high repetition rate XFEL and extreme light Facility (SHINE) project is designed to produce fully coherent X-ray photons covering the photon energy from 3 keV to 25 keV. We have reported our FEL proposal and schemes in the hard X-ray regime which is self-seeding based on the crystal monochromator previously. Comparing to the transmission self-seeding scheme, the reflection one has several advantages and might be the base proposal. Start-to-end (S2E) simulations from the beam generation by Astra, the linac accelerating by Elegant to the FEL simulation by Genesis are performed. In this manuscript, the FEL simulations based on the S2E beam will be presented mainly. The results demonstrate the feasibility of the reflection hard X-ray self-seeding at the SHINE project.

INTRODUCTION

Hard X-ray self-seeding FEL scheme based on a crystal monochromator was proposed and has been demonstrated that it is a practicable method to generate a fully coherent hard X-ray pulse. Currently, transmission and reflection modes are considered each FEL facility worldwide. The transmission mode [1] has been adopted more popular, such as LCLS [2], PAL-XFEL and European XFEL. The reflection mode is also feasible which has been used and demonstrated successfully at SACLA [3].

Both of the line FEL-1 and FEL-3 at SHINE will work on hard X-ray self-seeding FEL schemes for covering 5-15 keV (nominal 3-25 keV). In the previous papers [4, 5], the transmission case and the reflection case have been proposed and discussed, where both of the advantages and disadvantages were presented and compared. In some degree, the reflection case shows a higher monochromatic efficiency, a lower heat-loading, better signal-to-noise ratio and higher pulse energy.

In this manuscript, we will present a start-to-end simulation results. The tracked electron beam generated by Astra [6], and accelerated and transported by Elegant [7], is used for generation of hard X-ray FEL by Genesis [8] with typical photon energy of 12.4 keV at the line FEL-1, where SASE, single-stage self-seeding and two-stage self-seeding configurations are carried out.

REFLECTION SELF-SEEDING

As shown in Fig. 1, the layout of a two-stage reflection self-seeding scheme is presented here. Adopting two-stage scheme, one can decrease the heat-loading on the crystal, enhance the monochromaticity, and correct the beam offset of the s-polarized reflection.

The magnetic field centre of the second undulator section will be adjusted according to the beam offset. The second monochromator with opposite direction can make the trajectory back to the initial one. However, this method does not work on the gap-fixed undulator.

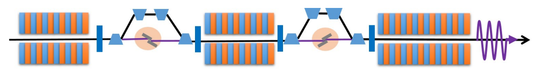

Figure 1: Layout of the two-stage reflection hard X-ray self-seeding scheme at the SHINE.

The basic double-crystal monochromator is shown in Fig. 2, where the layout consists of a channel-cut crystal and a beam stopper. The beam stopper is pressed against the right edge of the forward crystal which is used to block the SASE pulse transmitting the crystal. Refer to the normal monochromator of the beam line, smaller Bragg angle is used for higher energy photon. Typically, the C111 symmetric diamond crystal can cover 5-15 keV energy photons in the range of 11.6-37 degree Bragg angles. The channel-cut gap D is assumed as 100 μm. For the 12.4 keV photon, the Bragg angle of C111 is 14.1 degree and then the induced time delay is 162 fs and the transverse offset is 194 μm.

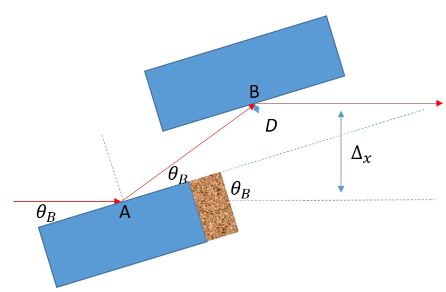

Figure 2: Reflection monochromator with double-crystal for self-seeding.

LINAC AND BEAM PARAMETERS

The schematic layout of the SHINE is shown in Fig. 3, which includes a 8 GeV accelerator and three FEL lines. In the baseline of the SHINE, an 100 MeV electron beam with 100 pC charge is generated in the photon-injector section and accelerated to 8 GeV at the exit of the linac. The peak current is more than 1500 A, the rms normalized slice emittance is less than 0.5 mm·mrad and the rms slice energy spread is less than 0.01%.

* Work supported by the National Natural Science Foundation of China Grant No. 11605277
† liutao@sinap.ac.cn;liutao@zjlab.org.cn

ISBN: 978-3-95450-210-3 doi:10.18429/JACoW-FEL2019-TUP087

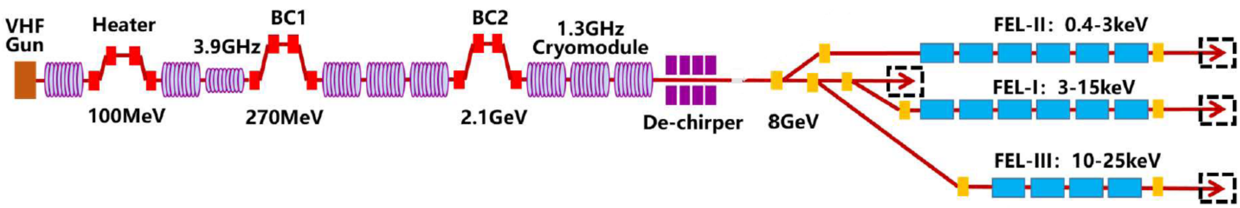

Figure 3: Schematic layout of SHINE.

Considering the 12.4 keV photon generated in the line FEL-1, the beam will be transport through the switchyard and matched at the entrance of the line FEL-1. Currently the S2E beam has been tracked from RF gun to the entrance of undulator using Astra and Elegant. Figure 4 shows the tracked beam properties.

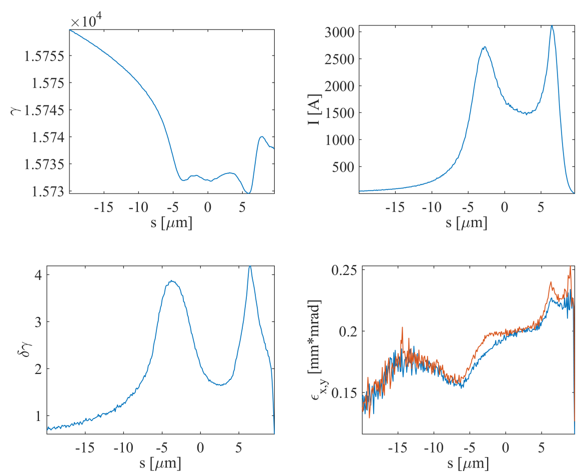

Figure 4: Sliced parameters of the tracked beam: Top-left: the sliced relative energy distribution. Top-right: the current profile. Bottom-left: the sliced relative energy spread. Bottom-right: the normalized emittance of x (blue) and y (red). Beam tail is at the left side of s coordinate axis.

The beam envelope of $s = 0$ position is matched for FEL radiation. Beam energy is 8039 MeV, peak current is 1730 A, both emittances of x and y are 0.2 mm·mrad and energy spread is 0.013%. Calculated by Xie's Model [9], the optimal Twiss parameters are $\beta_x = 18.05, \beta_y = 7.64, \alpha_x = -1.56$ and $\alpha_y = 0.67$. The matched results are shown in Fig. 5. It is noted that the mismatch and offset of the beam exist, that will impact on the radiation pulse performance.

FEL SIMULATIONS

The line FEL-1 has 43 undulator modules, where each module is a 4-m-long permanent magnet planar hybrid structure with 152 periods of $\lambda_u = 26$ mm and an adjustable magnetic gap. For such long undulator section, it can be used for SASE FEL well. We replaced the 7th module and the 13th module as the reflection monochromators for self-seeding schemes. Two-monochromator adoption is order

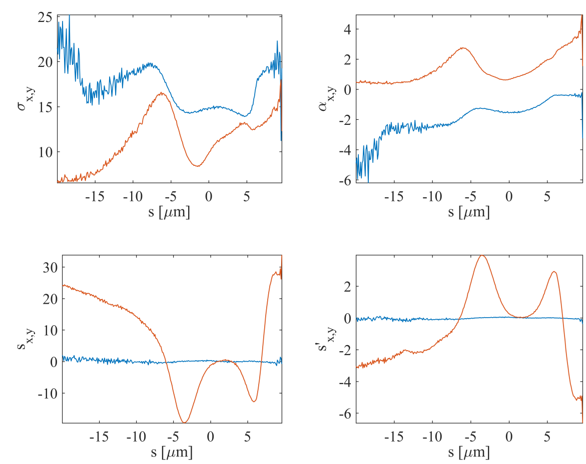

Figure 5: Twiss parameters of x (blue) and y (red) of the electron beam: Top-left:the sliced beam size. Top-right: the sliced $\alpha_{x,y}$. Bottom-left: the sliced transverse offsets. Bottom-right: the angular deviation. Beam tail is at the left side of s coordinate axis.

to decrease the heat-loading, improve the monochromaticity further and eliminate the sideband. Here both SASE and self-seeding FEL S2E simulations are carried out in the following.

SASE

Figure 6 presents the 12.4 keV SASE FEL performance in which undulator tapering is considered. It is noted that the exponential gain performs and stops at about 70 m with $\sim 130\mu$J (saturation). Due to undulator tapering, the FEL pulse energy increases continuously and is up to 1300 μJ and the peak power is 80 GW with bandwidth FWHM of 0.15% at the exit of the undulator section.

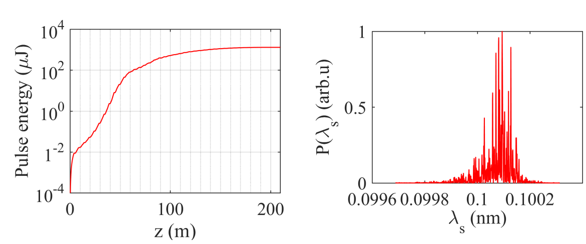

Figure 6: SASE. Beam tail is at the left side of s coordinate axis.

ISBN: 978-3-95450-210-3 doi:10.18429/JACoW-FEL2019-TUP087

Self-seeding

For the self-seeding scheme, both single-stage case and two-stage case are presented here. In order to decrease the heat-loading of the crystal, the first monochromator is placed at the 7th undulator module. Before the monochromator, the SASE pulse energy is about 0.3 μJ shown in Fig. 7.

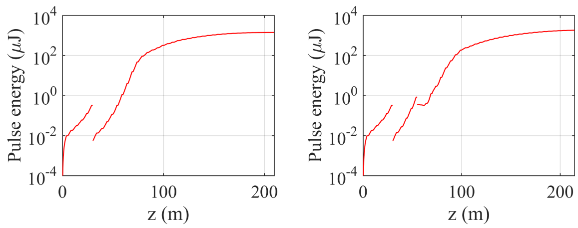

Figure 7: Pulse energy growth along the undulator for self-seeding schemes. Left: Single-stage self-seeding. Right: Two-stage self-seeding.

Figure 8 shows the single-stage self-seeding spectra evolution in both of the time and frequency domains. Before the monochromator, the SASE pulse with 10s MeV peak power, 0.3 μJ pulse energy and FWHM 0.5% bandwidth is generated. The monochromatization process is simulated by XOP [10]. A fully coherent radiation pulse with FWHM 6e-5 bandwidth and 0.3 MeV peak power is filtered out from the SASE pulse. In the seeding section downstream, the

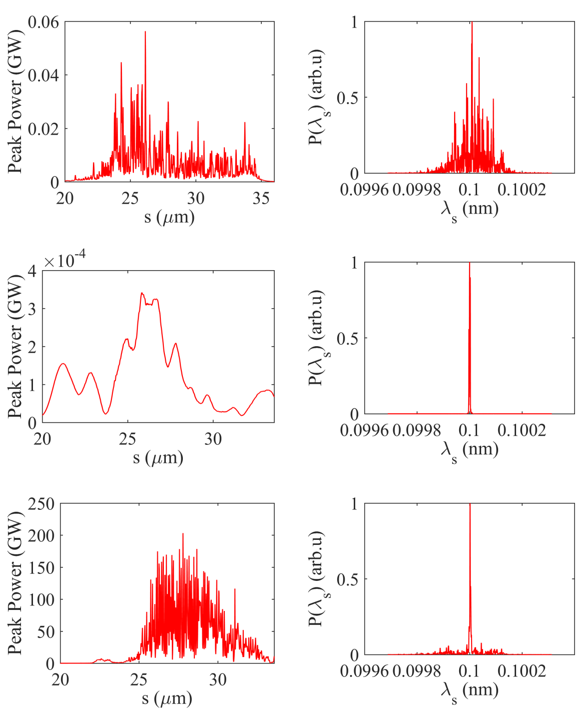

Figure 8: Spectra in the time domain and frequency domain for the single stage self-seeding. Top: Spectra before the monochromator. Middle: Spectra after the monochromator. Bottom: Final spectra after the single-stage self-seeding with tapered undulator.

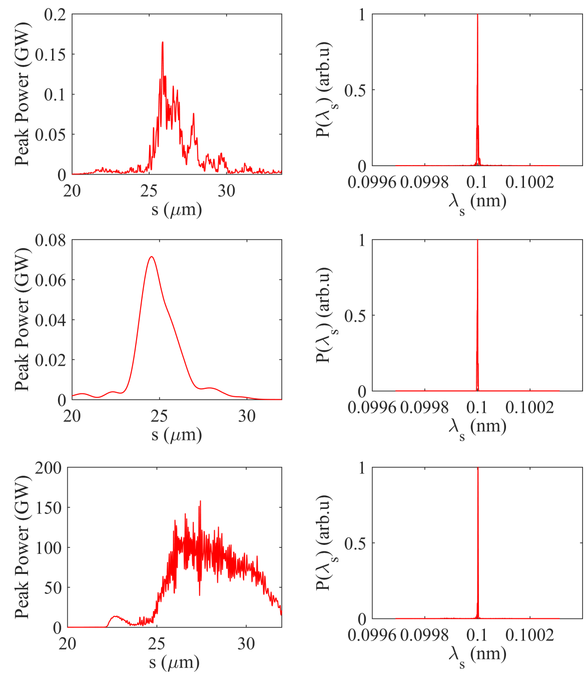

Figure 9: Spectra in the time domain and frequency domain for the two-stage self-seeding. Top: Spectra after the first self-seeding stage and before the second monochromator. Middle: Spectra after the second monochromator. Bottom: Final spectra after the two-stage self-seeding with tapered undulator.

pure radiation is high than the noise power of the beam, and will be amplified as the seed laser. Due to the long distance undulator section, tapering is also adopted and the final peak power is about 150 GW and the pulse energy is 1300 μJ. The bandwidth is less than 1e-4, but the sideband is considerable.

Figure 9 shows the two-stage self-seeding spectra evolution in both of the time and frequency domains. Firstly, we still use the same SASE section and the following monochromator as the single-stage case as shown in the top and middle of Fig. 8. After a 5 undulator modules section, the seeded FEL peak power is 100 MW, the pulse energy is 0.6 μJ and sideband starts appearing. At this time, the second monochromator works and a pure FEL pulse is filtered out with 70 MW peak power much higher than the beam noise. Similarly, the 70 MW seed laser is amplified to saturation quickly and further increases by tapering. The final peak power is 100 GW and the pulse energy is 1800 μJ. The spectra is still fully coherent with the bandwidth FWHM of 6e-5 and the sideband is invisible. It is illustrated that the result is much better is the single-stage case.

CONCLUSION

The S2E simulation presents the SASE, single-stage self-seeding and two-stage self-seeding results of 12.4 keV photon. For the SHINE project, the two-stage reflection self-seeding is feasible to generate fully coherent hard X-ray. Next step, we will design the reflection monochromator and test the photon energy range at the synchrotron radiation facility.

ISBN: 978-3-95450-210-3 doi:10.18429/JACoW-FEL2019-TUP087

ACKNOWLEDGEMENTS

The authors would like to thank for Bo Liu, Haixiao Deng and Dong Wang for helpful discussions and useful comments.

REFERENCES

[1] G. Geloni, V. Kocharyan, and E. L. Saldin, "A novel selfseeding scheme for hard x-ray FELs", *Journal of Modern Optics*, vol. 58, no. 16, p. 1391, 2011. doi:10.1080/09500340.2011.586473

[2] J. Amann *et al.*, "Demonstration of self-seeding in a hard-X-ray free-electron laser", *Nature Photonics*, vol. 6, p. 693, 2012. doi:10.1038/nphoton.2012.180

[3] I. Inoue *et al.*, "Generation of narrow-band X-ray free-electron laser via reflection self-seeding", *Nature Photonics*, vol. 13, p. 319, 2019. doi:10.1038/s41566-019-0365-y

[4] T. Liu *et al.*, "Optimization for the two-stage hard X-ray self-seeding scheme at the SCLF", in *Proc. IPAC'18*, Vancouver, BC, Canada, May. 2018, paper THPMK070, pp. 4460–4463. doi:10.18429/JACoW-IPAC2018-THPMK070

[5] T. Liu *et al.*, "Proposal of the reflection hard X-ray self-seeding at the SHINE project", in *Proc. IPAC'19*, Melbourne, Australia, May 2019, pp. 1792–1794. doi:10.18429/JACoW-IPAC2019-TUPRB047

[6] K. Flöttmann, *Astra - A Space Charge Tracking Algorithm*, http://www.desy.de/~mpyflo, 2000.

[7] M. Borland, *User's Manual for Elegant*, APS-ANL, Chicago, IL, 2017.

[8] S. Reiche, "GENESIS 1.3: a fully 3D time-dependent FEL simulation code", *Nucl. Instrum. Methods Phys. Res. A*, vol. 429, no. 1-3, p. 243, 1999. doi:10.1016/S0168-9002(99)00114-X

[9] M. Xie, "Design optimization for an X-ray free electron laser driven by SLAC linac", in *Proc. PAC'95*, Dallas, TX, USA, May 1995, paper TPG10, pp. 183–195.

[10] ESRF, X-ray Oriented Programs Software Package, https://www.aps.anl.gov/Science/Scientific-Software/XOP